Effect of Embedded Piezoelectric Sensors on Fracture Toughness and Fatigue Resistance of Composite Laminates Under Mode I Loading

American Society of Composites
21st Annual Technical Conference
September 17-20, 2006
Dearborn, MI

Gretchen B. Murri
U.S. Army Research Laboratory
Vehicle Technology Directorate
NASA Langley Research Center
Hampton, VA 23681

ABSTRACT

Double-cantilevered beam (DCB) specimens of a glass/epoxy composite material with embedded piezoelectric sensors were tested both statically and under fatigue loading to determine the effect of the embedded material on the Mode I fracture toughness and fatigue resistance compared to baseline data without the embedded elements. A material known as LaRC-Macrofiber Composite (LaRC-MFC™), or MFC, was embedded at the midplane of the specimen during the layup. Specimens were manufactured with the embedded MFC material either at the loaded end of the specimen to simulate an initial delamination; or with the MFC material located at the delaminating interface, with a Teflon film at the loaded end to simulate an initial delamination. There were three types of specimens with the embedded material at the delaminating interface: co-cured with no added adhesive; cured with a paste adhesive applied to the embedded element; or cured with a film adhesive added to the embedded material. Tests were conducted with the sensors in both the passive and active states. Results were compared to baseline data for the

same material without embedded elements. Interlaminar fracture toughness values (G_{Ic}) for the passive condition showed little change when the MFC was at the insert end. Passive results varied when the MFC was at the delaminating interface. For the co-cured case and with the paste adhesive, G_{Ic} decreased compared to the baseline toughness, whereas, for the film adhesive case, G_{Ic} was significantly greater than the baseline toughness, but the failure was always catastrophic. When the MFC was in the active state, G_{Ic} was generally lower compared to the passive results. Fatigue tests showed little effect of the embedded material whether it was active or passive compared to baseline values.

INTRODUCTION

Embedded piezoelectric materials, both active and passive, have been proposed as a means of adding multi-functionality, such as active shape-change, vibration control, and health monitoring for aircraft structures. Embedding the piezoelectric material in the structure can have advantages over surface bonding for some situations; e.g., protecting the actuation system from damage, preserving aerodynamic shape of an outer surface, or shape-changing in an interior location. However, embedding a foreign material in a laminated composite creates both material and geometric discontinuities, which can act as sources for delamination onset. Therefore, the viability of these embedded sensors for use in highly flexible structures depends on both the effect of the embedded element on the durability of

Gretchen B. Murri, U.S. Army Research Lab, Vehicle Technology Directorate, NASA Langley Research Center, Hampton, VA 23681.

the structure and the integrity of the embedded component under fatigue loading. In this study, coupon-level double-cantilevered beam (DCB) specimens with embedded elements were used to characterize the Mode I fracture toughness and fatigue resistance of the embedded sensor-to-composite bond in a glass/epoxy composite material. The embedded elements used were piezoceramic devices, produced using a process developed at NASA Langley. The Macro-Fiber Composite (LaRC-MFC™) manufacturing process yields high-performance flexible actuators at much lower cost compared to traditional piezocomposites. Details of the development and performance of LaRC-MFC™ are found in ref. 1. To date, the MFCs have been used successfully in several smart structure test programs at NASA Langley.

In ref. 2, the fatigue behavior of a graphite/epoxy laminate with an embedded piezoelectric (PZT) actuator was compared under mechanical and electromechanical loading. To embed the PZT material, an area with the dimensions of the PZT insert was cut out of the two center plies and the PZT was fit into the cut-out and the laminate was cured. Tension-tension fatigue tests on coupon specimens were conducted at a frequency of 10 Hz and an R-ratio of 0.1 at stress levels of from one-half to twice the design limit of the PZT. For the electromechanical loading, AC voltage was applied to the actuator, either ranging from -10 V to -100 V , or from 10 V to 100 V, at 10 Hz. This resulted in an electrically induced strain that was either in-phase (negative voltage) or out-of-phase (positive voltage) with respect to the mechanical loading. The embedded actuators had only a moderate decrease in fatigue life during the out-of-phase electromechanical testing, even at stress levels above the given operating range of

the PZT. However, for the in-phase electromechanical testing the fatigue life dropped sharply at stress levels above the design limit of the PZT. This was believed to be due to the PZT material being polarized by the negative AC voltage, as well as being depolarized by the mechanical fatigue loading.

In ref. 3, piezoelectric material (PZT) was embedded in a composite panel to investigate the effect on tension failure stress and tension-tension fatigue. The PZT material was either inserted into a cut-out area as in ref. 2, or directly inserted in the layup and co-cured. Both configurations, as well as specimens with no PZT were loaded in axial tension to failure. The failure stress and damage sequence were nearly identical for all three cases. Similarly, tension-tension fatigue loading of the same type specimens showed no difference in fatigue life for the specimens with embedded PZT. In these tests, the PZT material was not actuated.

In ref. 4, several material tests (Flatwise Tension, Double Lap Shear, Short Beam Shear, Quasi-Static Impact, and Plate Compression) were performed on specimens of four different composite material systems, embedded with a flexible material containing a network of distributed piezoceramic sensors. None of the tests showed a degradation of the integrity of the structure due to the embedded material.

Fracture-mechanics-based failure models are being used to study delamination problems in a variety of composite structures [5, 6]. Theses models require fracture toughness data for the modeled material systems. Therefore, in order to model systems with embedded elements, the effect of the embedded material on G_{Ic} must be understood. In this study, DCB specimens of S2/E773 glass/epoxy composite were used to evaluate the effect of embedded MFC material. Specimens were

manufactured using two designs, either with the MFC material at the loaded end, acting as the delamination starter; or with a Teflon delamination starter at the loaded end, and the MFC at the delaminating interface. In two sets of specimens, an adhesive was added to the MFC-to-composite interface.

EXPERIMENTS

Materials and Specimens

The MFC material used consists of three primary components: a sheet of aligned piezoelectric fibers in epoxy, a pair of thin polymer films etched with a conductive electrode pattern, and an adhesive matrix material to bond the parts together. A complete MFC unit is shown in Fig. 1. The thicknesses of the active and inactive regions, shown in Fig. 1(b), were nominally 0.0115 inches and 0.0063 inches, respectively. Table I lists properties for the MFC material. To create material for embedding in the DCB specimens, strips of MFC were manufactured, each strip having 12 separate "cells". The width of the active region of each cell was approximately 0.79 inches and there was 0.2 inches of inactive material between the cells to allow for cutting the specimens. The units were nominally 3.7 inches long. A photo of an MFC strip is shown in Fig. 2.

To create the test specimens, 12-inch-square unidirectional panels were manufactured from S2/E773 glass/epoxy material. Material properties are listed in Table II. The panels were 22 plies thick and had the embedded materials placed at the midplane at the edges of the panels, allowing the ends with the pin connectors to extend beyond the edges of the panels. Figure 3 shows a photograph of a cured panel, using backlighting to show the areas with the embedded MFC material, and

the pin connections at the left and right edges. After curing, the panels were cut down the center, and then each half was cut using a very fine saw blade between the circuit packs, along the lines shown on Fig. 3. Each panel yielded 24 specimens, each approximately 1 inch wide by 6 inches long.

Figure 4(a) shows a sketch of a typical DCB specimen. The laminate contains a thin non-adhesive insert (such as 0.0005 inch Teflon film) at the midplane at one end, to simulate an initial delamination. Load is applied as shown, at the end with the insert and a delamination grows along the midplane toward the other end. For this study, specimens were created with the typical DCB geometry with the addition of the MFC material. Two different panel types were manufactured. For the first case, configuration B, the MFC was placed at the loaded end of the specimen and acted as the delamination starter, or insert material. A sketch of this specimen type is shown in Fig. 4(b). A sheet of 0.0005 inch Teflon was added on each side of the MFC material to ensure that the MFC did not bond to the composite. In the second configuration (configuration C), the MFC was added at the delaminating interface, as shown in Fig.4(c), with Teflon alone used as the insert material. Additionally, there were three variations of configuration C, regarding the MFC-to-composite bond. In the first configuration, C1, the MFC was simply co-cured with the panel, with no added adhesive. However, in order to ensure that a good bond was achieved between the MFC and composite, two other configurations with added adhesive were made: C2, in which a paste adhesive (Hysol EA956) was applied to both sides of the MFC during layup; and C3, which used a film adhesive (3M AF 163-2) applied to the MFC during layup. Table III lists the adhesive properties, obtained from the manufacturers' literature. For these panels, two pieces of Teflon

film were used at the insert end, with the ends of the Teflon slightly overlapping each side of the inactive material at the end of the MFC. Although the two Teflon sheets were the same size, sometimes they did not end at the same exact location in the specimens, due to shifting during the manufacture process.

For one specimen of the C1 type, the edge was polished and the area at the delamination front was inspected. Figure 5 shows a photomicrograph of the region where the Teflon films meet the MFC and overlap it slightly on both sides. Although the end of the insert is difficult to see in the figure, there was no noticeable resin pocket at the end of either of the Teflon films, resulting in a reasonably sharp delamination front in these specimens.

Figure 6 shows a photograph of the polished edge of a C2 specimen at the region where the Teflon insert ends. As the photo shows, most of the C2 specimens had a large bead of the paste adhesive near the end of the MFC material. However, in all these specimens, the Teflon film overlap extended around this bead, with the end of the Teflon in the region of constant adhesive thickness. Figure 6 also shows areas where bubbles formed in the adhesive in the bead and along the length of the MFC. The thickness of the adhesive at the end of the Teflon was 0.014 inch for this specimen. In order to determine whether this thickened adhesive region extended across the width of the specimen, the specimen was cut lengthwise down the center and the interior edge was polished. A photomicrograph of the interior edge is shown in Fig. 7. This figure shows that, in addition to the bead at the end of the MFC, the thickness of the paste adhesive also varies along the length of the MFC in the interior.

A specimen of configuration C3 (with film adhesive) was also polished, and the area at the delamination front was examined. Figure 8 shows the edge of a typical C3 specimen. The adhesive film increases in thickness from the tip of the Teflon until it reaches a constant thickness in the active region of the MFC material. In these specimens, the Teflon overlapped the film adhesive for only 0.04 to 0.08 inches, or, the end of the Teflon film formed a wrinkle at the end near the adhesive, as indicated in the figure. For this example, the thickness of the adhesive is approximately 0.007 inch at the delamination front (end of the Teflon), increasing to 0.014 inch at the end of the MFC inactive region. This specimen was also sectioned down the centerline and polished. The interior edge had the same appearance as that shown in Fig. 8.

In addition to the specimens manufactured for this study, some specimens from a panel of S2/E773 without embedded MFC elements were tested to determine baseline values of G_{Ic} for comparison with the MFC specimens. The baseline specimens were tested in the same fixtures and using the same procedures and data reduction.

Test Procedures

Prior to testing, piano hinges were bonded to the insert end of the specimens to allow the load application. In order to make the delamination easier to see, a thin coat of white paint was applied to the edges of the specimen. A strip of tape, marked in 0.039 inch (1 mm) increments was also attached to the edge of the specimen, with the end of the tape aligned with the end of the insert. Figure 9 shows a specimen in the test set-up, with the piano hinges gripped in the test machine. All tests were conducted under displacement control in a small table-top

servo-hydraulic test stand using a 50-lb load cell. The tests were controlled by a computer program, which also recorded the test data. A video camera with a close-up lens with a magnification of 4X was used to monitor the delamination growth, and the image was displayed on a television screen.

In order to test specimens in the active state, a signal generator and voltage amplifier system were used. The signal generator produced a sine wave with a frequency of 1 Hz. The voltage amplifier then multiplied the voltage by a factor of 1000 and transferred it to the MFC. To conduct a test with active MFC, the specimen was placed in the test fixture, the voltage was gradually increased from 0 to the desired level, and then the load was applied. The target value for the voltage signal was a maximum of 1500 volts and minimum of -500 volts for all tests. This is the recommended operating range of the MFC material and corresponds to strain levels of between 1500 and -500 με within the MFC actuator. However, for some specimens, it was necessary to use lower peak levels to avoid arcing in the MFC material. All tests were conducted with the minimum voltage equal to -500 volts, and the maximum between 1200 and 1500 volts. There was no detectable movement of the DCB specimens with the MFC activated.

Static Tests

Static tests were conducted according to ASTM Standard D 5528-01 [7]. Displacement was applied at a rate of 0.1 in/min. As the displacement was applied, load (P) and crosshead displacement (δ) were continually recorded by the computer. As the delamination grew, each 0.039 (1 mm) inch of growth observed on the marking tape was recorded on the load-displacement record by means of a keystroke on the computer. Delaminations were typically allowed to grow to 2

inches. Tests were also video-recorded for review during the data analysis. A typical load-displacement record for configuration C1 is shown in Fig. 10. For each static test, in addition to the maximum load point (P_{max}), the point at which the P-δ curve becomes non-linear (P_{NL}) was determined, by fitting a line to the straight part of the initial P-δ curve.

After completing the test, the specimen was removed from the fixture and broken completely open. The exact initial delamination length, *a*, the distance from the load application point to the end of the insert, was then measured from the delaminated surface and recorded. The fracture toughness, G_{Ic}, was calculated using the modified beam theory method [7] and P_{NL} results.

Fatigue Tests

Fatigue tests were used to generate a delamination onset threshold curve, according to the procedure in ASTM Standard 6115-97 [8]. The fixtures and apparatus used were the same as those used for the static tests. In order to generate a complete curve over a range of cycles, tests were run at a variety of G_{Imax} levels. Test values were chosen as a percentage of G_{Ic} and the associated δ_{max} for each test was calculated from

$$\frac{\delta_{max}^2}{[\delta_{cr}]_{avg}^2} = \frac{G_{Imax}}{G_{Ic}}$$

where δ_{cr} is the average of the critical displacements from the static tests for a given specimen type.

Prior to each fatigue test, the specimen was statically loaded to the calculated δ_{max} to determine the initial compliance of the specimen and then unloaded. Fatigue

testing was then conducted using a frequency of 5 Hz and an R-ratio of 0.1. The computer program recorded the cycle count, maximum and minimum load, and maximum and minimum displacements, as well as the calculated compliance (C) at a specified interval, usually every 10 cycles. Cyclic tests were run until C had increased by 5% over the initial value, or until a maximum number of cycles was reached without the 5% compliance change (called a runout).

RESULTS

Static Tests – Passive

Figure 11 shows a summary of the G_{Ic} results for each configuration compared to baseline results for specimens of S2/E773 without embedded MFC. A minimum of five specimens was tested for each configuration. The error bars show the range of the data for each configuration. Results are shown for specimens tested for this study, as well as results from a separate study performed at the Materials and Engineering Research Lab (MERL) in England [9]. The fracture toughness values were almost identical for both labs – 0.80 in-lb/in^2 for this study and 0.79 in-lb/in^2 at MERL. There was also very little scatter in the data. Delamination growth in the baseline specimens was very stable and easy to track during the testing.

For configuration B (MFC as the insert), Fig. 11 shows that the average G_{Ic} value, 0.85 in-lb/in^2, was slightly higher than the baseline results. Delamination growth in these specimens was also stable and easy to track. There is more scatter in this data, as shown by the error bars in Fig. 11, compared to the baseline data. Extensive fiber bridging was observed for configuration B. Figure 12 shows the R-curves for these specimens. The increasing toughness with delamination growth is

a result of the fiber bridging. For the configuration C specimens, fiber bridging was prevented by the presence of the MFC at the delaminating interface. Therefore there was no R-curve effect observed for configuration C.

For configuration C1 (MFC at the midplane, co-cured with no additional adhesive), average G_{Ic} was about 30% lower than the baseline value, (0.54 in-lb/in^2). For these specimens, the delamination growth was usually stable but, in some cases, would occur in "jumps" of 0.2 to 0.4 inches. In two of the 6 tests, the delamination growth began at one interface between the MFC and composite, but then changed to the other interface, causing the MFC to split across the width during the test. There was no R-curve effect in any of the configuration C specimens since fiber bridging was prevented by the presence of the MFC material,

Results for the configuration with paste adhesive, C2, gave an average G_{Ic} value that was less than half the baseline value (0.37 in-lb/in^2). The C2 specimens showed stable growth in general, with the delamination growing within one of the adhesive layers (cohesive failure). Figure 13(a) shows a typical failure for the C2 specimens, where the delamination apparently grew within one of the adhesive layers along the entire length, leaving a coating of adhesive on both sides of the fracture surface. In one test of a C2 specimen, the initial delamination growth from the Teflon film occurred between the adhesive and MFC on one surface and then the delamination transitioned to the other adhesive layer, tearing the MFC material near the Teflon. The resulting G_{Ic} for that specimen was 0.84 in-lb/in^2, just above the baseline value. Figure 13(b) shows a photo of the fracture surface for that specimen. Figure 13(c) shows a schematic of the edge view of the delamination

growth, first at the interface above the MFC, then tearing through the MFC and growing the rest of the way through the adhesive below the MFC.

Figure 11 also shows that there is much more scatter in this data set compared to configuration B, or the baseline results. The reduced G_{Ic} results, as well as the increased variability in the results, may be an effect of the voids in the adhesive, observed in Fig. 6. Although the adhesive layer is fairly thick at the delamination front, these voids in the adhesive could reduce the strength of the bond, resulting in a reduction in measured toughness.

The C3 laminates always failed catastrophically with the delamination growing almost the entire length of the specimen. The resulting G_{Ic} values were much higher than any of the other configurations, as shown in Fig. 11. In an attempt to get delamination growth data from these specimens, a controlled-precrack technique was used to create a sharp delamination front in the specimen. Steel blocks were clamped on the specimen at distances of 0.04 to 0.12 inches in front of the insert, and the specimen was loaded in the test fixture until a delamination had grown to the blocks. The clamp and blocks were then removed and the specimen was re-loaded to failure. The secondary failures were also catastrophic in every test and yielded toughness values comparable to the tests from the insert. No delamination growth data could be generated for this configuration. It is possible that the thick zone of adhesive at the delamination front in these specimens is the reason for the large increase in the toughness. Because of the length of this adhesive region (see Fig. 8) from the Teflon to the MFC material, the precracking did not extend the delamination tip beyond this adhesive area but, in fact only, to an area of even thicker adhesive.

Static Tests – Active

A minimum of five static tests were performed for each specimen type with the MFC in the active state. Maximum applied voltage for each specimen was between 1500 and 1200 volts; minimum voltage was -500 volts. Figure 14 shows a comparison of the passive and active results for each case, along with the baseline results shown by the solid line. For configuration B, when the MFC material was acting as the insert, there was a slight drop (about 6.5%) in G_{Ic} when the MFC was active, as shown in the figure. However, active tests of the specimens with the MFC co-cured at the midplane (configuration C1) resulted in values of G_{Ic} that were significantly higher than the passive results and higher than the baseline values. There was also a difference in the delamination growth behavior of these C1 specimens. For the passive tests, delamination growth was generally stable and easy to track, as noted previously, with only an occasional unstable jump in delamination length. However, when the MFC was in the active state, the delamination growth occurred entirely in jumps of from 0.2 to 0.8 inches at a time. Figure 15 shows a typical load-displacement curve for the C1 specimens with active MFC. Each drop in load indicates a jump in delamination length.

Results for the C2 specimens with active MFC were about 12% lower than the results in the passive condition and much lower than the baseline value. The delamination grew within the adhesive layer, as it did for the specimens with passive MFC, and the growth was very stable.

The C3 specimens with active MFC failed in the same manner as the C3 passive specimens (catastrophically) and resulted in lower G_{Ic} values compared to the passive tests. The controlled-precrack technique was also attempted with these

specimens with the same result as in the passive case. Various precrack lengths were used, but no stable delamination growth could be achieved. Toughness values, shown in Fig. 14, were reduced approximately 10% for the active condition compared to the passive results. Both the active and passive conditions resulted in a very large amount of scatter in the data sets for the C3 specimens.

Fatigue Tests

Fatigue tests were conducted using configurations B and C1 in the passive and active states. The C2 specimens were tested only active. Tests were run at G_{Imax} levels of 50, 40, and 30% of G_{Ic}. As specified in ref. 8, specimens were cycled until the compliance had increased by 5%. Figure 16 shows results for the tested specimens, as well as baseline data for S2/E773 from ref. 9. Right-pointing arrows on the data indicate runouts, where the testing was stopped with no delamination growth detected. The average G_{Ic} values are also shown on the y-axis for each case. The results for configurations B and C1 fall into the range of the baseline data. There also does not seem to be any notable difference between the passive or active results for these configuration types. Results for the C2 specimens are lower than for the other cases. This is consistent with the low static G_{Ic} values for this configuration.

There was never any damage observed to the MFC material throughout the fatigue testing. When the MFC was activated, a wave-like motion could be observed in the unsupported MFC material. All specimens with active MFC were checked visually at the end of testing to determine whether the MFC was still functioning. The MFC proved to be very durable, lasting through the longest fatigue test (8 million cycles).

The addition of the adhesives to the C2 and C3 panels did not seem to be beneficial in these tests. The C2 specimens were found to have an uneven adhesive thickness, as well as multiple voids in the adhesive that probably caused them to fail prematurely. Conversely, the C3 specimens had a large area of adhesive at the delamination front, which increased in thickness as it approached the end of the MFC material. This likely resulted in the greatly increased G_{Ic} values for that specimen type. Therefore, neither of these tests (C2, C3) is a good measure of the effect of embedded material itself on the fracture toughness or fatigue life of this composite material.

CONCLUSIONS

Static and cyclic DCB tests were conducted on a glass/epoxy laminate with embedded piezoelectric elements (MFC) at the midplane. The MFC was either at the insert end of the specimen or at the delamination interface. When the MFC material was at the delaminating interface, it was either simply co-cured with the embedded material; or a paste, or film adhesive was applied to the embedded MFC material. All configurations were tested under static loading to determine G_{Ic} in both the active and passive states. Results were compared to baseline values for the test material. Three configurations were tested under cyclic loading to determine delamination onset values, in the passive and active states. The following results were observed:

1. The addition of the MFC material at the insert end of the specimen changed G_{Ic} only slightly compared to the baseline value for the passive and active

cases. Using the MFC as the delamination starter did not cause the delamination to grow prematurely.

2. For the passive tests, embedding the MFC at the delaminating interface caused a decrease in G_{Ic} for the co-cured and paste adhesive configurations.
3. For the passive tests of the film adhesive specimens, G_{Ic} was significantly increased over the other configurations, although the failure was catastrophic. Precracking the specimens before testing did not achieve stable growth.
4. The effect of making the MFC active was varied. For the co-cured case with the MFC at the delaminating interface, G_{Ic} went up by 53% compared to the passive case. For all the other configurations, G_{Ic} went down by from 6% to 12% compared to the passive case.
5. Fatigue results showed no effect of either the presence of the embedded material, or whether it was passive or active. Results for the specimens with paste adhesive were noticeably lower than the other cases, but those results are consistent with the reduced G_{Ic} for that configuration.
6. The MFC material remained intact and functioning throughout the longest fatigue tests. However, in some of the static tests the material tore across the width during loading.

Based on the results of this study, embedding the MFC material does not appear to cause significant reductions in fracture toughness or fatigue resistance when the MFC is co-cured with the laminate. Since co-curing resulted in a good bond between the MFC and composite, additional adhesive was not necessary. In fact,

added adhesives resulted in significantly reduced or increased toughness values, due to manufacturing defects or artificially thick adhesive pockets – conditions that are unrelated to the effect of the presence of the MFC. In the tests conducted for this study, the MFC was very durable, both structurally and in electrical performance.

REFERENCES

1. Wilkie, K., R. G. Bryant, J. W. High, R. L. Fox, R. F. Hellbaum, A. Jalink, Jr., B. D. Little, and P. H. Mirick. 2000. "Low-Cost Piezocomposite Actuator for Structural Control Applications," presented at the SPIE 7th Annual International Symposium on Smart Structures and Materials, Newport Beach, CA, March 5-9, 2000.
2. Mall, S. and T. L. Hsu. 2000. "Electromechanical fatigue behavior of graphite/epoxy laminate embedded with piezoelectric sensor/actuator," in *Smart Materials and Structures*, 9, 2000, pp. 78-84.
3. Mall, S. 2002. "Integrity of graphite/epoxy laminate embedded with piezoelectric sensor/actuator under monotonic and fatigue loads," in *Smart Materials and Structures*, 11, 2002, pp. 527-533.
4. Lin, M. and F. K. Chang. 2002. "The manufacture of composite structures with a built-in network of piezoceramics," in *Composites Science and Technology*, 62, 2002, pp.919-939.
5. Murri, G. B., T. K. O'Brien, and C. Q. Rousseau. 1998. "Fatigue Life Methodology for Tapered Composite Flexbeam Laminates," in *Journal of the American Helicopter Society*, April 1998, pp.146-155.

6. Krueger, R., I. Paris, T. K. O'Brien, and P. J. Minguet. 2000. "Fatigue life methodology for bonded composite skin/stringer configurations," in *Journal of Composites Technology and Research*, 24, 2000, pp. 56-79.
7. ASTM Standard D5528-01, Standard Test Method for Mode I Interlaminar Fracture Toughness of Unidirectional Fiber-Reinforced Polymer Matrix Composites, ASTM International, 100 Barr Harbor Drive, West Conshohocken, PA.
8. ASTM Standard D6115-01, Standard Test Method for Mode I Fatigue Delamination Growth Onset of Unidirectional Fiber-Reinforced Polymer Matrix Composites, ASTM International, 100 Barr Harbor Drive, West Conshohocken, PA.
9. Martin, R., P. Hansen, T. Elms, and K. Potterill. 2001. DCRD Phase 2 Materials Data. Materials Engineering and Research Laboratory Ltd. (MERL), Hertford, U. K., BHTI-DCRD/4 Rev C, 2001.
10. O'Brien, T. K., G. B. Murri, R. Hagemeier, and C. Rogers. 1995. "Combined Tension and Bending Testing of Tapered Composite Laminates," in *Applied Composite Materials*, 1, 1995, pp. 401-413.

TABLE I. MATERIAL PROPERTIES OF LARC-MFC™ [1]

	Thickness, inches inactive/active region	E_1, psi	E_2, psi
LaRC-MFC	0.0063/0.0115	5.0×10^6	1.1×10^6

TABLE II: S2/E773 MATERIAL PROPERTIES [10]

Property	S2/E773
t_{ply}, inch	0.0093
E_{11}^t, Msi	7.38
E_{22}, Msi	1.76
G_{12}, Msi	0.83
ν_{12}	0.280

TABLE III. ADHESIVE PROPERTIES AT ROOM TEMPERATURE (PER ASTM D 638).

	Ultimate strength, psi	Tensile modulus, psi	Poisson's ratio
Hysol EA956 (paste)	6900	3.6×10^5	
3M AF 163-2 (film)	7000	1.6×10^5	0.34

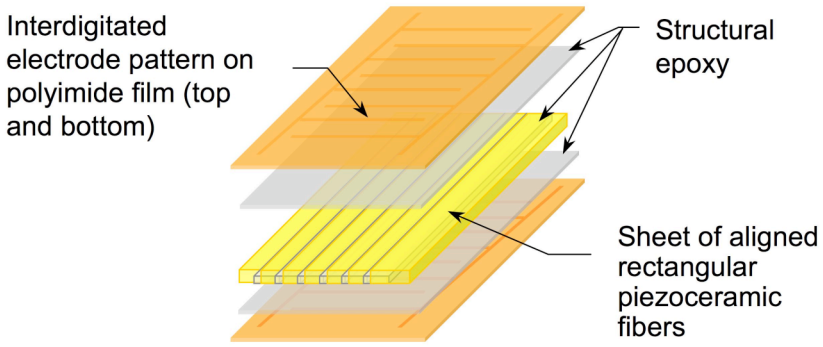

(a)Langley Macro-Fiber Composite™ actuator components.

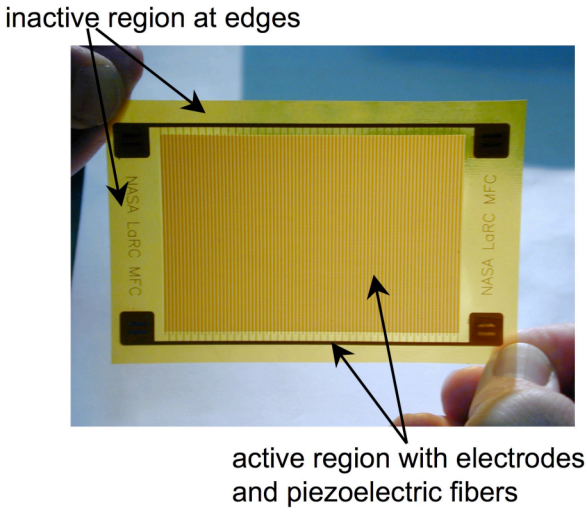

(b) Completed Langley Macro-Fiber Composite™ actuator.

Figure 1. LaRC -MFC composite actuator assembly and final product [1].

Figure 2. Strip of MFC cells for embedding in composite laminate.

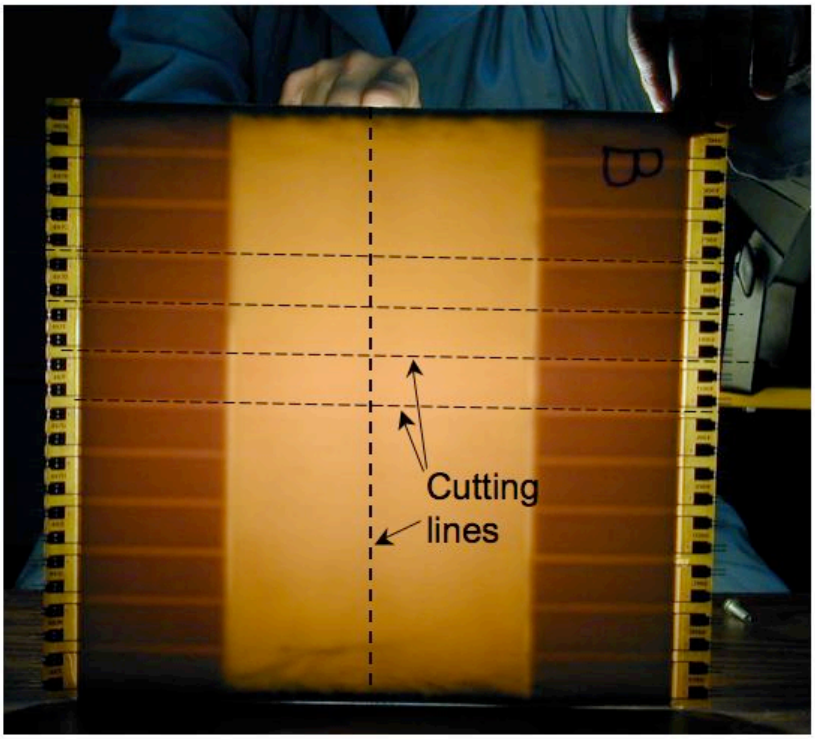

Figure 3. Cured composite panel with embedded MFC cells.

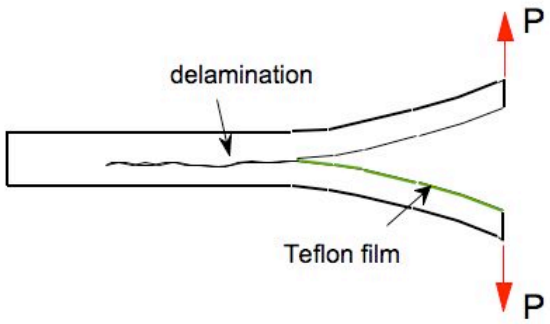

(a) standard double-cantilevered beam (DCB) specimen

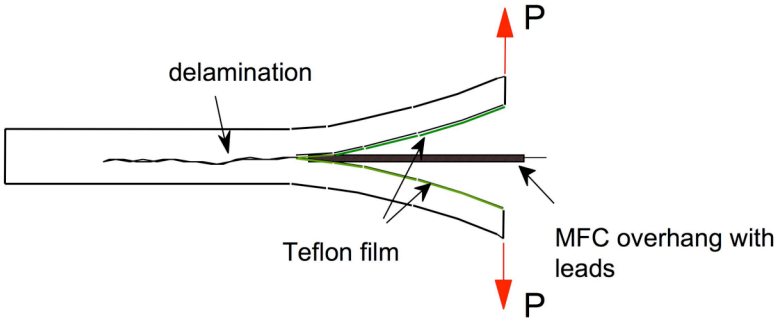

(b) DCB specimen with MFC as the insert material

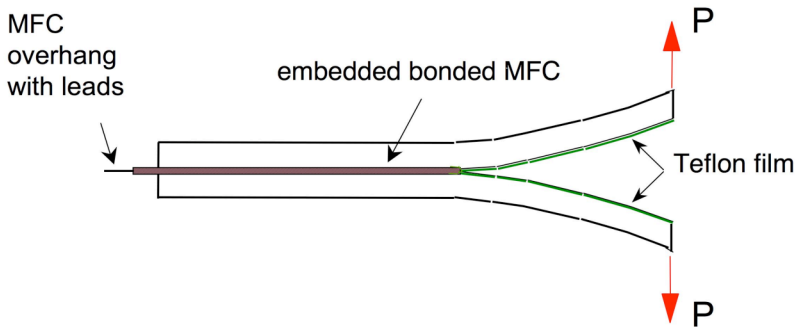

(c) DCB specimen with MFC at the delaminating interface

Figure 4. Standard and modified DCB specimen designs.

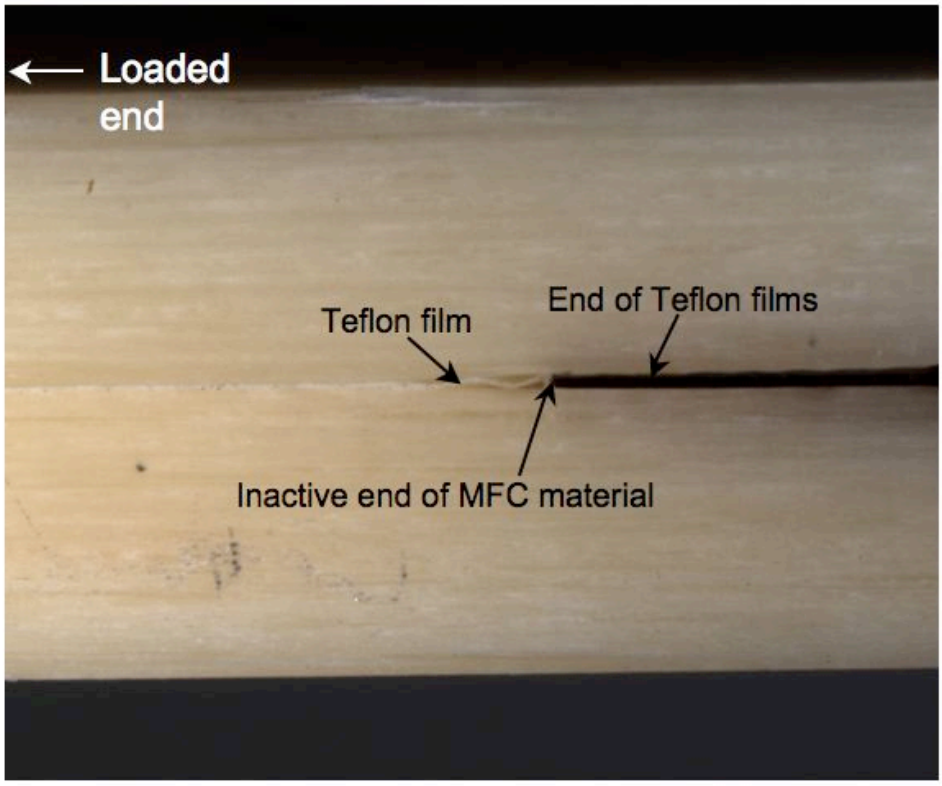

Figure 5. Edge of C1 specimen showing Teflon film and MFC material.

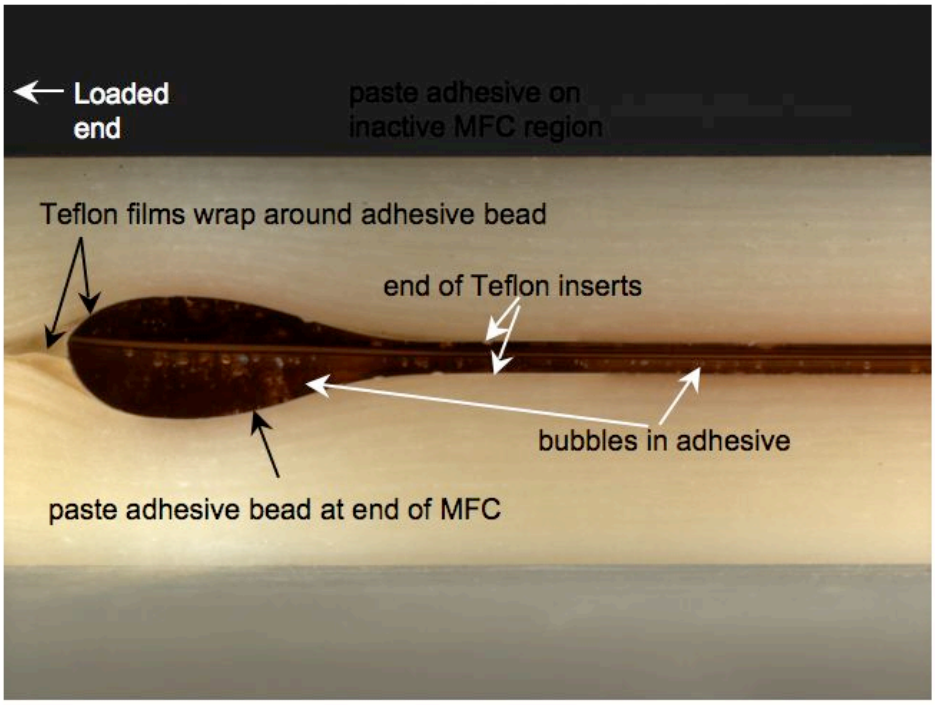

Figure 6. Edge of C2 specimen, showing adhesive bead and bubbles in adhesive.

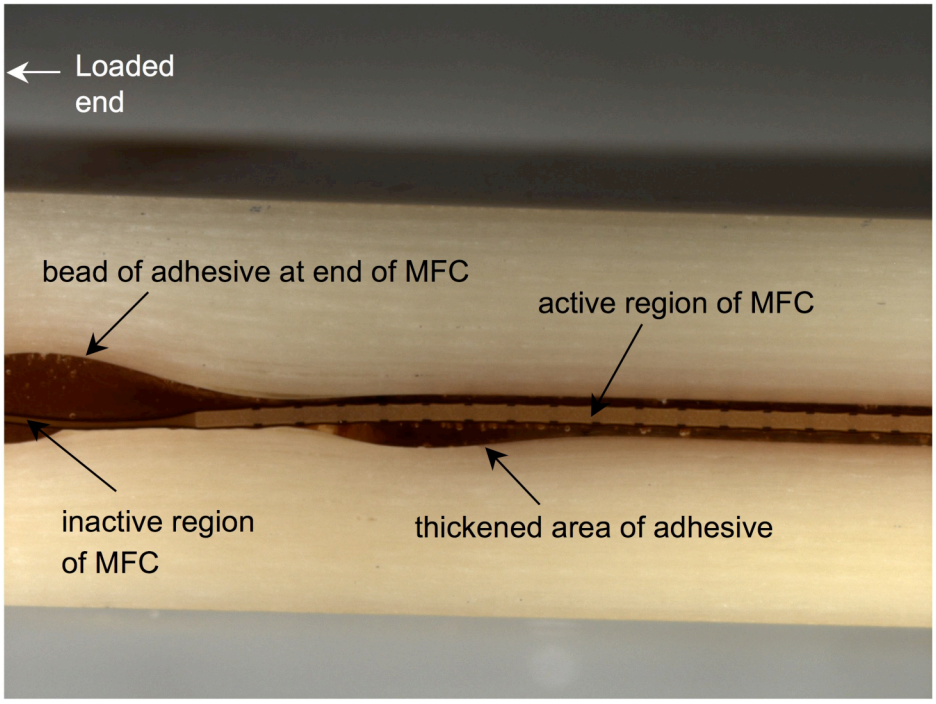

Figure 7. Photomicrograph showing uneven thickness of paste adhesive along MFC material.

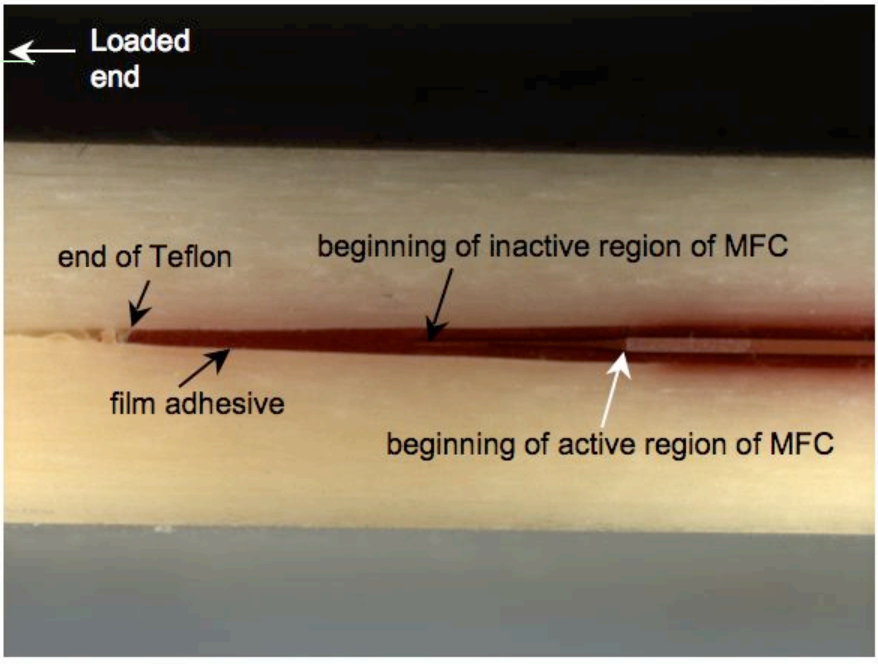

Figure 8. Edge photomicrograph of C3 specimen,

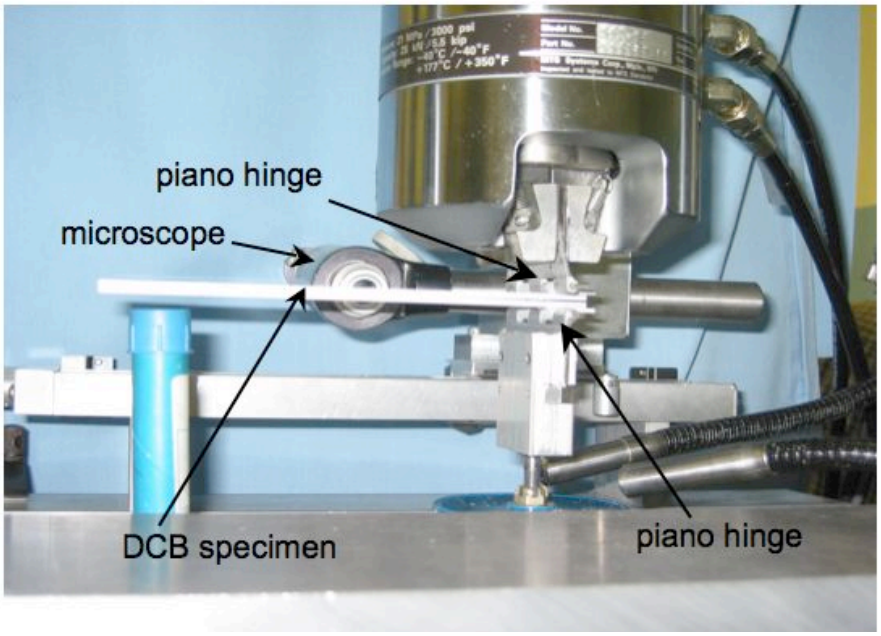

Figure 9. DCB specimen in loading fixture.

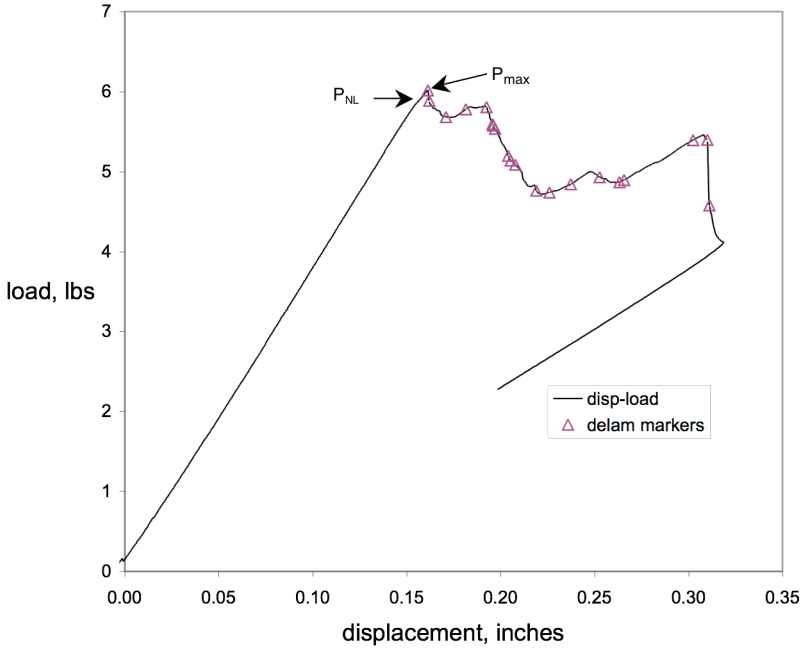

Figure 10. Load-displacement plot for static test of configuration C1 with embedded MFC material.

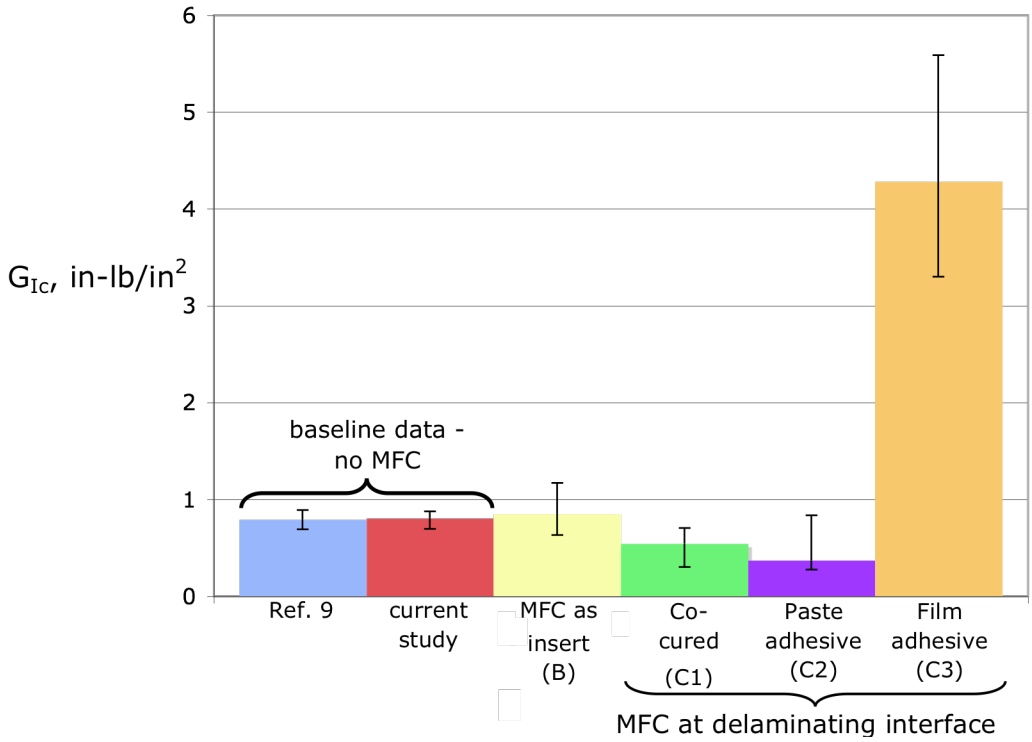

Figure 11. Static G_{Ic} average results for DCB specimens with and without embedded MFC material.

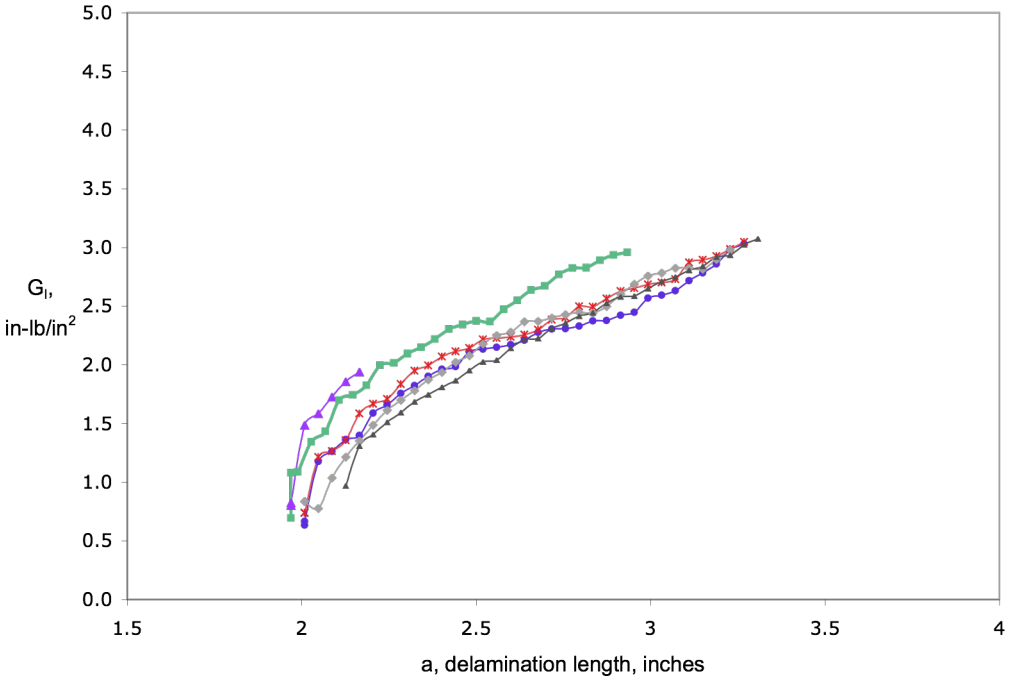

Figure 12. Delamination resistance curve (R-curve) for configuration B specimens.

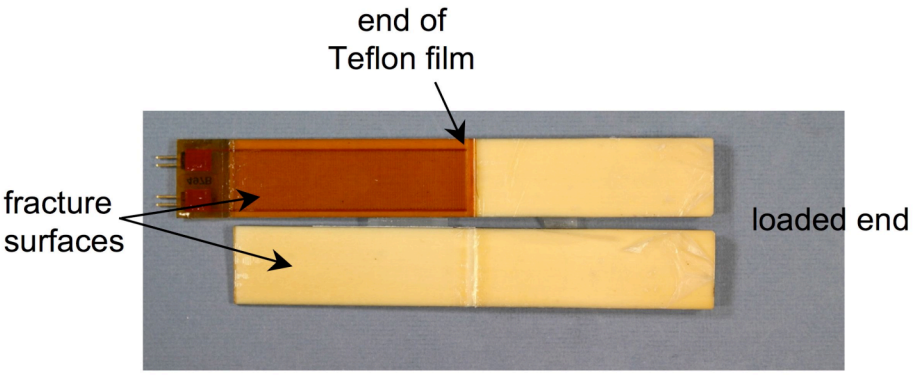

(a) Typical fracture surface of C2 specimen with paste adhesive applied to MFC material.

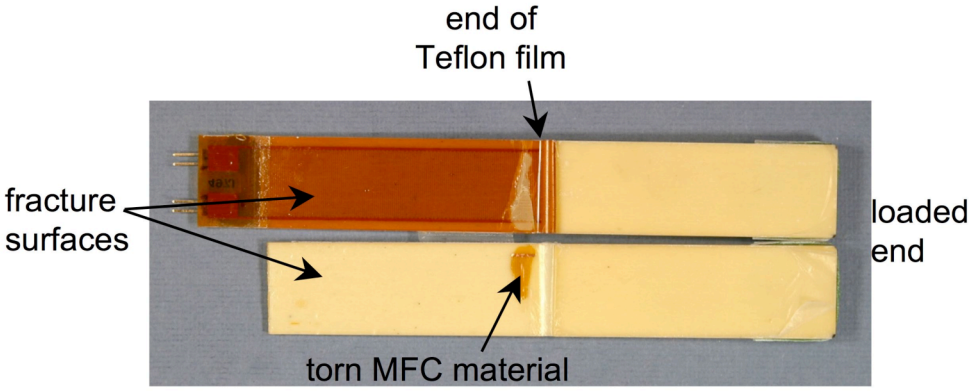

(b) Fracture surface in C2 specimen. Delamination path cut across MFC material from one adhesive surface to the other.

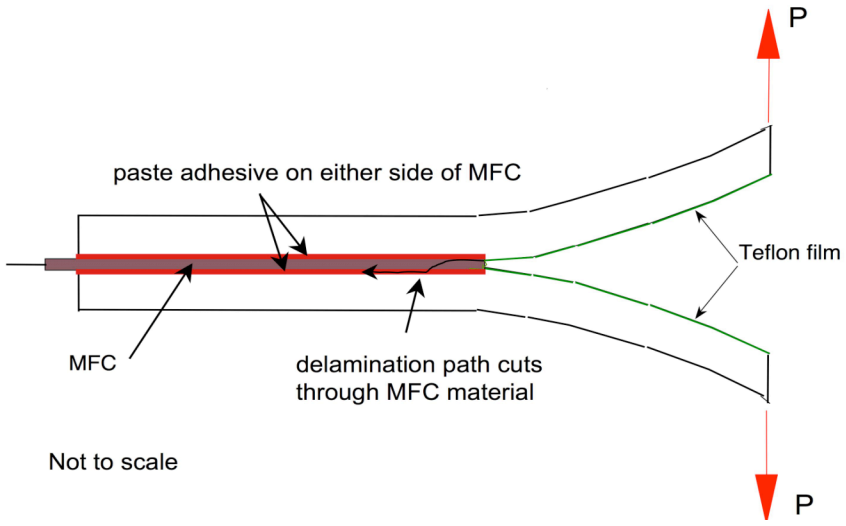

(c) Sketch of edge view of delamination path in specimen shown in 13(b).

Figure 13. Fracture surfaces of C2 specimens.

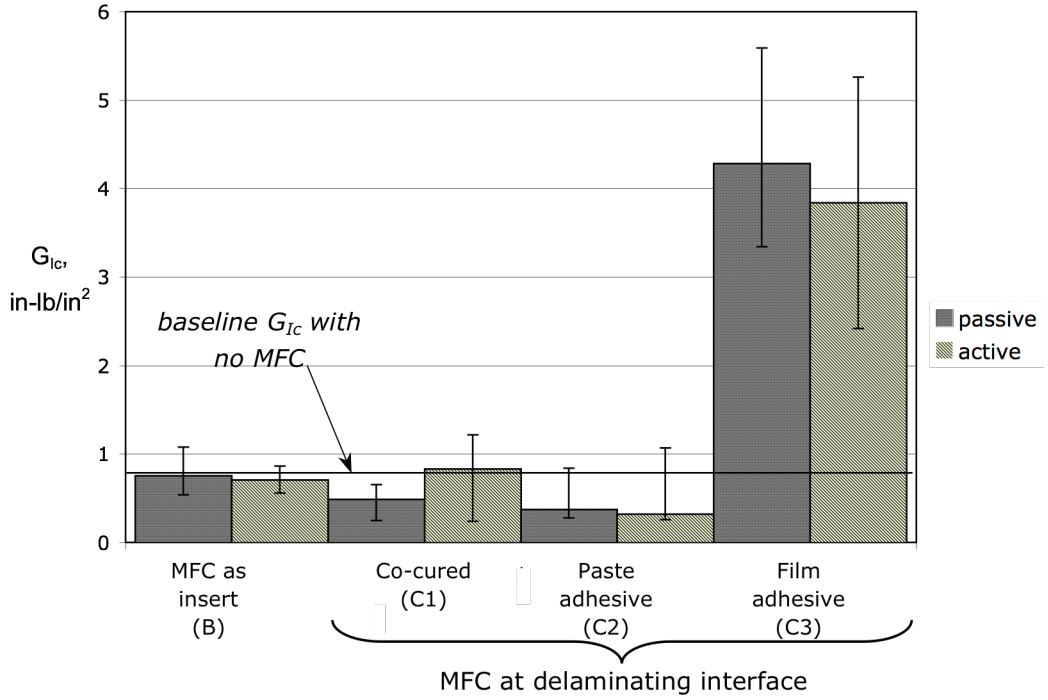

Figure 14. Average G_{Ic} results for DCB specimens with embedded MFC material in the passive and active states.

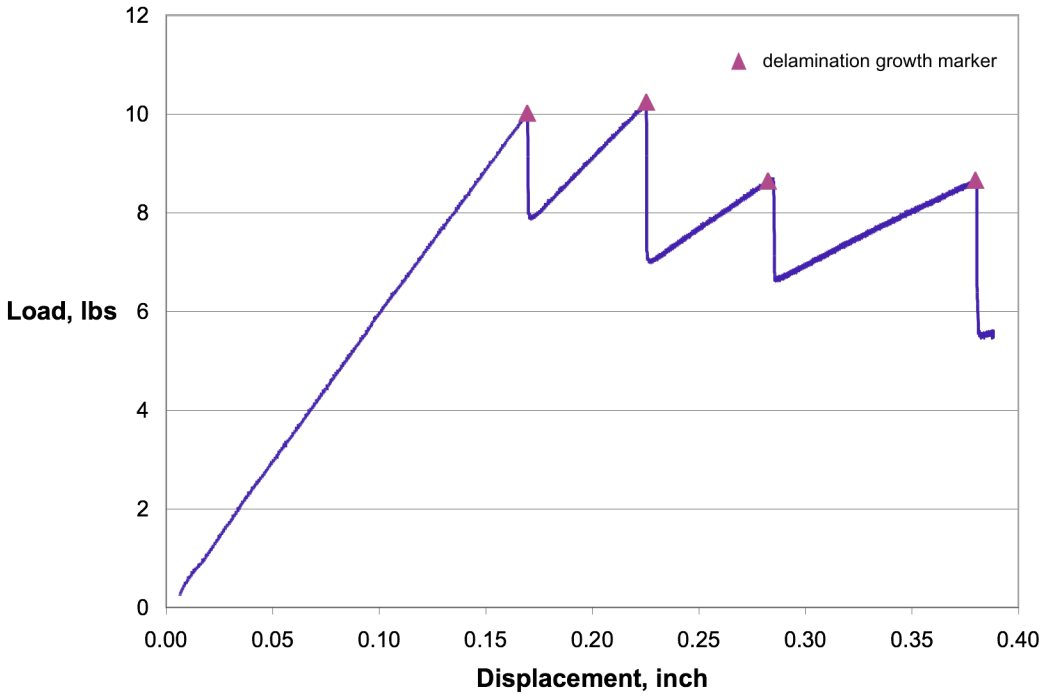

Figure 15. Typical delamination growth plot for a static test of a configuration C1 specimen with active MFC.

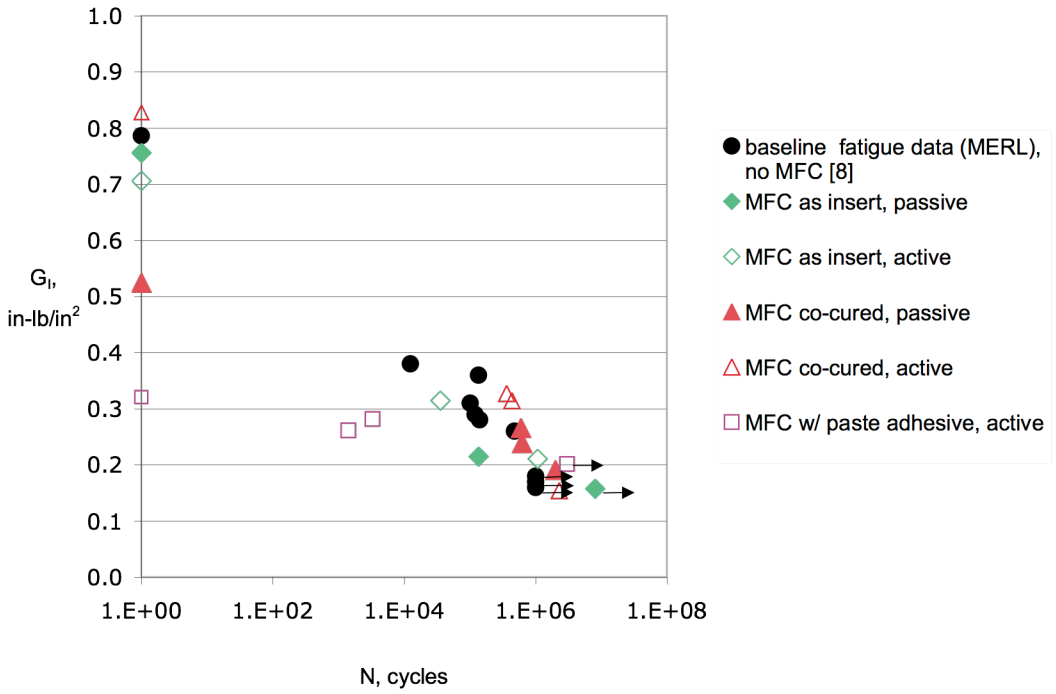

Figure 16. Delamination onset results for specimens with embedded MFC elements, active and passive conditions.